N95- 11018

BALLOON-BORNE MEASUREMENTS OF THE ULTRAVIOLET FLUX IN THE ARCTIC STRATOSPHERE DURING WINTER

Cornelius Schiller, Martin Müller, Erich Klein, and Ulrich Schmidt
Forschungszentrum Jülich, Institut für Atmosphärische Chemie
P.O. Box 1913, D-5170 Jülich, F.R. Germany

Ernst-Peter Röth
Universität Essen, Institut für Physikalische Chemie, F.R. Germany

ABSTRACT

Filter radiometers sensitive from 280 to 320 nm and from 280 to 400 nm, respectively, were used for measurements of the actinic flux in the stratosphere. Since the instruments are calibrated for absolute spectral sensitivity the data can be compared with model calculations of the actinic flux. Data were obtained during seven balloon flights during the European Arctic Stratospheric Ozone Experiment (EASOE).

1. INTRODUCTION

Photodissociation caused by the ultraviolet solar radiation is an important process controlling the chemistry of many short lived species in the stratosphere. E.g., the photolysis of ozone by solar radiation at wavelengths below 320 nm

$$O_3 + h\nu \rightarrow O(^1D) + O_2 \quad (\lambda < 320\ nm) \quad (1)$$

provides the major source of excited $O(^1D)$ atoms which generate OH which in turn initiate many oxidation processes in the atmosphere. The partitioning of NO_x species is forced by photochemistry, e.g. the photodissociation of NO_2:

$$NO_2 + h\nu \rightarrow NO + O(^3P) \quad (\lambda < 400\ nm) \quad (2)$$

The diurnal variation of chlorine species in the stratosphere is also a result of photodissociation by ultraviolet light as the photodissociation of the ClO dimer, HOCl, Cl_2, OClO, BrCl, $ClONO_2$, and others.

In order to interpret measurements of these key species in the stratosphere, usually photodissociation frequencies calculated by radiative models are used. In this paper, a measurement technique is presented which enables in-situ observations needed to validate model calculations of photoactinic fluxes in the stratosphere as well as the interpretation of simultaneous measurements of short lived species. Measurements using this technique were carried out during seven balloon flights during the Arctic winter in the course of the European Arctic Stratospheric Ozone Experiment (EASOE) in 1991/92.

2. EXPERIMENTAL

Filter radiometers to measure the photoactinic flux were developed in our laboratory, mainly for tropospheric use (Junkermann et al., 1989; Brauers and Hofzumahaus, 1992). They are equipped with an optical input system gathering radiation from 2π sr solid angle in order to achieve a sensitivity independent of the direction of incident radiation. The radiation is detected by UV-phototubes. The spectral sensitivity of the radiometers is defined by optical filters and the sensitivity of the phototubes.

In order to study different photochemical processes, radiometers sensitive at two different wavelength intervals were used: Figure 1 shows the spectral sensitivity of the UV-B radiometer which is equipped with an interference filter of 12 nm full width at half maximum peaking at 300 nm and a solar blind phototube (Hamamatsu R 1384). As discussed previously (Junkermann et al, 1989), it is essential to use a solar blind detector in combination with a highly blocking interference filter to suppress radiation from longer wavelengths and hence to be sensitive in the UV-B spectral region only. Instead of photomultiplier tubes which are used for the instruments for tropospheric measurements, the balloon-borne instruments are equipped with phototubes with a subsequent electrometer amplifier with an amplification factor of 10^9 to 10^{11}. They have the same spectral sensititvity, however, and they provide substantial lower weight. The instruments are temperature stabilized in order to avoid a thermal drift of the dark current and a spectral shift of the transmission of the interference filter.

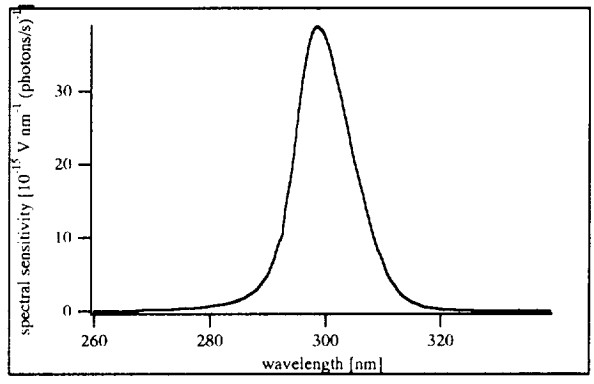

ig. 1. Absolute spectral sensitivity of the UV-B radiometer on the photon flux

The sensitivity of the second type of radiometers ranges from 280 to 400 nm. The radiation is detected by an UV-photodiode (Hamamatsu R 488-2) in combination with filter glass (Schott UG11). The spectral sensitivity is shown in Figure 2. The exact shape of the sensitivity curve at wavelengths below 280 nm is uncertain, but due to the low

number of photons these wavelengths make an unsignificant contribution to the overall signal of the radiometer.

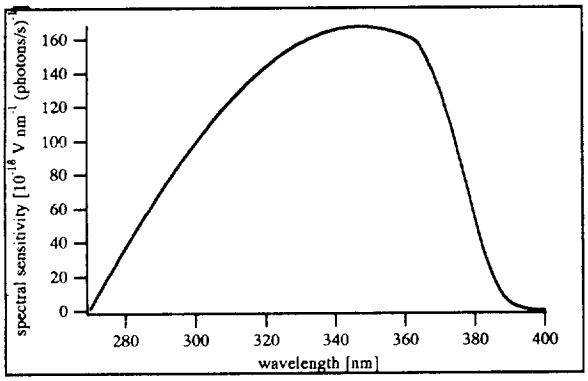

Fig. 2. Absolute spectral sensitivity of the near UV radiometer on the photon flux

During a balloon flight, four instruments are mounted on a gondola, one of each type gathering radiation from the upward hemisphere and from the downward hemisphere, respectively (Figure 3a). This configuration enables the separate measurement of the upward and the downward component of the photon flux. Although the instruments are mounted outside of the main gondola shadowing by the other experiments and by the suspension of the payload occurs. Due to the rotation of the gondola the direct incidence of sunlight is often inhibited. Therefore, the data have to be processed with regard to this shadowing as discussed below. During some flights, only one instrument of the near UV type (280 - 400 nm) was mounted piggy back on the balloon payload gathering light between 15° above the horizon and the earth (Figure 3b). For high zenith angles occuring at the twilight conditions during EASOE the directly incoming sunlight can be detected during each turn of the gondola when the instrument points towards the sun.

The data are recorded by an on-board data logger and can be - as an option - additionally transmitted to the ground station. The four instruments are integrated together with this computer and the power supply in a thermically isolated box. The mass of the entire box is 20 kg.

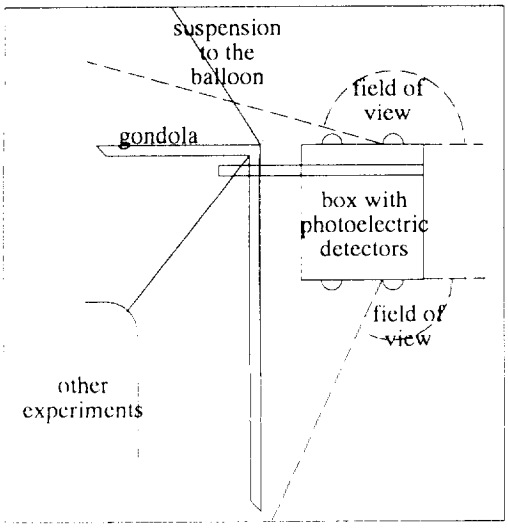

Fig. 3a. Mounting of the box with four radiometers

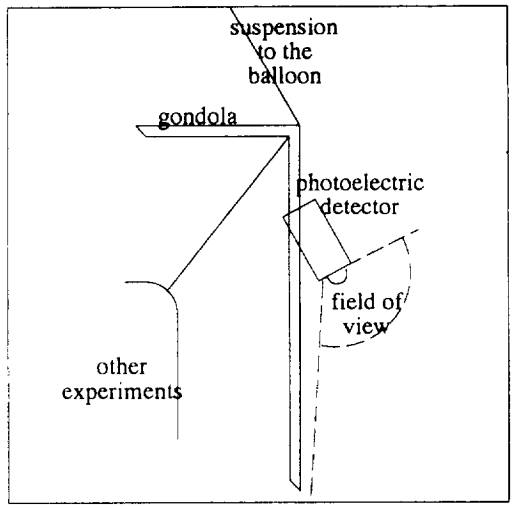

Fig. 3b. Mounting of a single radiometer on the gondola

3. CALIBRATION

The instruments can be calibrated in two ways: First, they can be calibrated for absolute spectral sensitivity on the incoming photon flux which is the suitable calibration for a comparison with model calculations of the solar flux. Secondly, the instruments can be calibrated for photodissociation frequencies which provides an independent check of the first calibration method and allows a direct comparison with measurements of trace gases.

3.1 Calibration for absolute spectral sensitivity

The relative spectral sensitivity $r(\lambda)$ of the radiometers was determined using a spectrograph and a tungsten halogen lamp. $r(\lambda)$ was corrected for the spectral characteristic of the system spectrograph-lamp which was measured using a calibrated photodiode.

In a second step, the signal U of the instruments was measured when exposed to the broadband radiation of an absolutely spectrally calibrated tungsten halogen lamp:

$$U = A \cdot \int r(\lambda) \cdot I(\lambda)\, d\lambda \qquad (3)$$

$I(\lambda)$ is the spectral irradiance of the calibrated tungsten halogen lamp incident to the detector and A is the factor which refers the relative sensitivity $r(\lambda)$ to the absolute sensitivity $S(\lambda)$ of the detector:

$$S(\lambda) = A \cdot r(\lambda) \qquad (4)$$

Hence the absolute sensitivity can be determined for each radiometer calculating the integral in (3) and measuring U.

In Figure 1 and 2, $S(\lambda)$ of an UV-B and a near-UV instrument are presented. For the UV-B instrument, the relative sensitivity $r(\lambda)$ of both the upward and the downward pointing radiometer agree nearly for all wavelengths. In the UV-B spectral region, significantly lower intensity of the upward flux which includes the direct radiation from the sun only at zenith angles higher than 90° is expected. Therefore, the electronic amplification of the radiometer pointing to the bottom whose spectral sensitivity is shown in Figure 1 exceeds that of the radiometer measuring light from the upper

hemisphere by a factor of 20. The absolute sensitivity of the radiometers of the near-UV type is approximately the same for all instruments used during EASOE, and the relative spectral sensitivity among one another is shifted by less than 1 nm.

3.2 Calibration for photodissociation frequencies

Using a calibration of the radiometers against a chemical actinometer, an independent check of the calibration for absolute spectral sensitivity can be carried out when simulating the signals of the photoelectric detectors with model calculations of the solar flux as described below and comparing them with photodissociation frequencies calculated with the same algorithm.

The spectral sensitivity of both types of radiometers is adapted to photoactinic spectra, that of the UV-B instrument to the photoactinic spectrum $P_1(\lambda)$ of ozone yielding $O(^1D)$ via reaction (1) and that of the near UV instrument to the photoactinic spectrum $P_2(\lambda)$ of NO_2 (reaction (2)). The photoactinic spectra $P_1(\lambda)$ and $P_2(\lambda)$ are defined by the product of the absorption cross section of ozone and NO_2, respectively, and the quantum yield of the corresponding reaction. For the ideal case, if the spectral sensitivity $S(\lambda)$ of the radiometers depends linearily on the photoactinic spectrum $P_1(\lambda)$ or $P_2(\lambda)$ for all wavelenghts λ

$$S(\lambda) = \text{const} \cdot P(\lambda) \tag{5}$$

the signal of the detector U becomes linearily dependent on the photodissociation frequency PF

$$U = \int S(\lambda) \cdot F(\lambda)\, d\lambda = \text{constant} \cdot \int P(\lambda) \cdot F(\lambda)\, d\lambda = \text{constant} \cdot PF \tag{6}$$

$F(\lambda)$ is the photon flux of the sun.

For several reasons the matching between $S(\lambda)$ and $P(\lambda)$ can be realized only approximatively and hence relation (5) becomes valid only for a limited wavelength interval or for specific experimental conditions. In the case of the UV-B detector, for zenith angles smaller than 85° light below 295 nm contributes to the $O(^1D)$ production via (1) in the stratosphere at which wavelengths (5) is no longer valid for the detectors used. Moreover, $P(\lambda)$ is a function of the temperature due to the dependence of the quantum yield in particular for reaction (1) which cannot be compensated by $S(\lambda)$. Therefore, the factor between the signal U and the photodissociation frequency in equation (6) becomes a function of several parameters as the temperature and the solar flux and hence the zenith angle and the column abundance of ozone.

Nevertheless, in a first approximation the signals of both types of radiometers can be related directly to photodissociation frequencies of reaction (1) and (2), respectively. The calibration factors will be determined by comparison with chemical actinometers (Junkermann et al, 1989; Hofzumahaus et al., 1992) this summer and be characterized for the corrections discussed above.

4. MODEL CALCULATIONS OF THE SOLAR FLUX

For the simulation of the signals of the photoelectric detectors two different models are in use. For a first interpretation of the measurements during the campaign, a fast but less accurate algorithm is applied. This model is based on a three beam approximation and was developed to run on a personal computer. A description of this model is can be found in Röth (1992).

The final simulation of the signals of the radiometers is carried out with a multi beam model which runs on a Cray XMP (Röth et al., 1992). This model calculates up to 20 different beams of the solar flux each representing the diffusive light in a cone shell distinguished by their angles against the vertical. The model is based on a line-by-line algorithm with a variable spacing between the considered wavelengths. In the UV-B spectral region, the spacing is less than 1 nm.

The model first calculates the collimated beam coming directly from the sun. This direct radiation is diminished by absorption by O_2, O_3, and NO_2, by Rayleigh scattering on air molecules and by Mie scattering on aerosols and cloud droplets. With these absorption and scattering processes, the direct photon flux F_d is given by Beer-Lambert's law

$$dF_d = -(\tau_{abs} + \tau_{scat}) \cdot F_d \cdot ds \tag{7}$$

with ds the pathlength within a given layer d, and τ the optical depth of the layer.

The photons are scattered into the different diffusive beams according to a phase function P_{ij}. The fluxes of these beams are also decreased by absorption and scattering. But, in contrast to the direct radiation, they gain photons by the scattering processes from the other rays. Thus, a source function term Q has to be added to the Beer-Lambert's law

$$dF_i = -(\tau_{abs} + \tau_{scat}) \cdot F_i \cdot ds_i + Q_i \cdot ds_i \tag{8}$$

with

$$Q_i = \sum_j F_j \cdot \tau_{scat} \cdot P_{ij} \cdot \frac{\mu_i}{\mu_j} \tag{9}$$

and μ_i the cosine of the individual zenith angle.

The differential equation system can be solved for one layer of thickness Δz if it is assumed that the layer is homogeneous in respect to the absorbing and scattering processes. Additionally, the source function should be constant within the layer which is realistic if the thickness does not exceed 1 km. As the source function couples the different fluxes the integrated equation system has to be solved by an iterative method.

The multi beam model has the advantage that it determines the actinic flux incident on the radiometers from different directions. Therefore, it is possible to simulate the signals of the radiometers looking upwards and downwards, respectively (Figure 3a), even if their field of view is slanted against the vertical (Figure 3b).

The algorithm calculates the radiation considering full spherical geometry including refraction. This feature is important in order to calculate photon fluxes at high zenith angles during twilight at which most of the measurements were carried out.

Exactly the same algorithms used to simulate the measurements can be applied for determining photodissociation coefficients. Therefore, if the signals of the radiometers are represented correctly by the model, the photodissociation frequencies calculated with the same program should be correct likewise as far as the photoactinic parameters of the species are known.

5. FIELD MEASUREMENTS

During the European Arctic Stratospheric Expedition (EASOE) in the winter 1991/92 the instruments were flown on seven balloon flights launched from Kiruna (68°N, 22°E)

listed in Table 1. Data were obtained for zenith angles between 68° and 95° up to altitudes of 32 km. The instruments were operated successfully during all flights. The data of the EASOE missions will be presented by Schiller et al. (1992).

date	configuration	max. altitude	zenith angles
Dec 5, 91	1 near UV	25 km	93° - 89°
Jan 22, 92	1 near UV	30 km	95° - 87°
Jan 31, 92	1 near UV	32 km	95° - 84°
Feb 5, 92	2 UV-B 2 near UV	33 km	84° - 95°
Mar 5, 92	1 near UV	30 km	94° - 79°
Mar 12, 92	2 UV-B 3 near UV	29 km	71° - 73°
Mar 20, 92	2 UV-B 2 near UV	32 km	68° - 82°

Tab. 1. Balloon missions of the filter radiometers during EASOE 91/92 including the number of instruments used, the maximum altitude, and zenith angles at which measurements were made.

5.1 Evaluation of the measured data

As an example, Figure 4 shows unprocessed data of a near UV radiometer taken every 2 seconds during the balloon flight on December 1991 together with the flight profile versus the flight time. Due to the rotation of the gondola which occurs on time scales of one to ten minutes, the signals are strongly influenced by shadowing and possibly also by reflected light from the gondola. At least during the ascent and during the descent when the frequency of the rotation of the gondola is high, an upper and a lower envelope on the data points can be identified: The upper limit shows the contribution of the direct incidence of radiation including the diffusive flux, and the lower limit represents signals with the direct radiation blocked out providing information on the diffusive actinic flux separately.

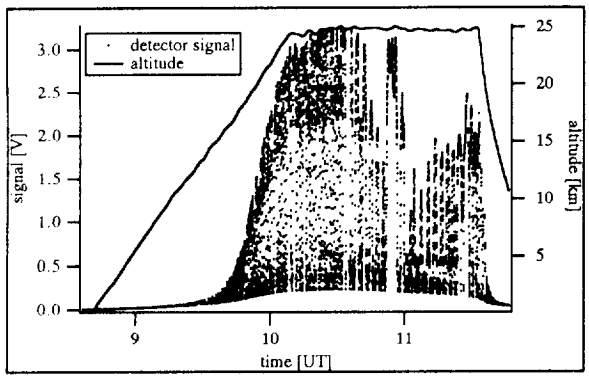

Fig. 4. Raw data of the near UV radiometer measured during the balloon flight on December 1991 together with the flight profile versus the flight time

For the evaluation of the measurements a program was designed which allows for separate determination of the signal's mean as well as of its upper and lower limits. By this procedure data which are influenced by shadowing or by reflected light from other experiments aboard the gondola can be omitted. Therefore, the data are evaluated several times resulting in 30 sec average values for the upper and the lower boundary of the signal omitting disturbed data points.

5.2 Planned data interpretation

The available data set of actinic fluxes allows a detailed examination of radiative processes in the stratosphere. Due to the wide range of zenith angles and altitudes at which measurements were accomplished a broad test of the photon flux models can be carried out, e.g. with regard to the ratio of direct to diffusive fluxes. Since most of the measurements are accomplished at zenith angles higher than 80°, a validation of the model in particular for twilight conditions at which modelling of photon fluxes becomes difficult will be done (Schiller et al., 1992). When simulating the measurements by model calculations, the influence of various parameters as the solar zenith angle, the ozone profile, the ground albedo, and the aerosol content on the actinic fluxes and hence on photochemistry can be studied. In particular for those flights during which species were measured whose concentration is driven by photochemistry, the interpretation using photodissociation frequencies with regard to the actual flight conditions is possible. From the link between the measurements and the model, we expect to calculate photodissociation frequencies for many atmospheric species more accurately. In forthcoming papers, we will publish a detailed analysis of the data with respect to these questions.

ACKNOWLEDGEMENTS

As part of EASOE, funds for the field measurements were granted by the CEC contract STEP-CT-91-0138. We would like to thank the CNES balloon launch team to launch the payloads under the difficult Arctic winter conditions. Integration of the instruments on the payloads of P. Aimedieu, R. Borchers, and C. Camy-Peyret is gratefully acknowledged We thank A. Engel, H. Franken, and G. Kulessa for their help during the field measurements and D. H. Ehhalt, A. Hofzumahaus, and U. Mörschel for many discussions.

REFERENCES

Brauers, T. and A. Hofzumahaus: Latitudinal variation of measured NO_2 photolysis frequencies over the Atlantic ocean between 50°N and 30°S. J. Atmos. Chem., 15, 269-282, 1992.

Hofzumahaus, A., T. Brauers, U. Platt, and J. Callies: Latitudinal variation of measured O_3 photolysis frequencies $J(O^1D)$ and primary OH production rates over the Atlantic ocean between 50°N and 30°S. J. Atmos. Chem., 15, 283-298, 1992.

Junkermann, W., U. Platt, and A. Volz-Thomas: A photoelectric detector for the measurement of photolysis frequencies of ozone and other atmospheric molecules. J. Atmos. Chem., 8, 203-227, 1989.

Röth, E.-P.: A fast algorithm to calculate the photonflux in optically dense media for use in photochemical models. Ber. Bunsenges. Phys. Chem., 96, 417-420. 1992.

Röth, E.-P., S. Johänning, and H. London: Description of a photonflux model to determine photodissociation coefficients. Ber. Forschungszentrum Jülich, in preparation, 1992.

Schiller, C., M. Müller, and E.-P. Röth: Ultraviolet actinic flux in the stratosphere: 3. Comparison of measurements during the European Arctic Stratospheric Ozone Experiment with model calculations. Geophys. Res. Lett., submitted, 1992.